



This is the accepted manuscript made available via CHORUS. The article has been published as:

Hadronic production of the doubly heavy baryon Ξ_{bc} at the LHC

Jia-Wei Zhang, Xing-Gang Wu, Tao Zhong, Yao Yu, and Zhen-Yun Fang

Phys. Rev. D **83**, 034026 — Published 23 February 2011

DOI: [10.1103/PhysRevD.83.034026](https://doi.org/10.1103/PhysRevD.83.034026)

Hadronic Production of the Doubly Heavy Baryon Ξ_{bc} at LHC

Jia-Wei Zhang, Xing-Gang Wu,* Tao Zhong, Yao Yu, and Zhen-Yun Fang

Department of Physics, Chongqing University, Chongqing 400044, People's Republic of China

We investigate the hadronic production of the doubly heavy baryon Ξ_{bc} at the large hadron collider (LHC), where contributions from the four (bc) -diquark states $(bc)_{\bar{3},6}[^1S_0]$ and $(bc)_{\bar{3},6}[^3S_1]$ have been taken into consideration. Numerical results show that under the condition of $p_T > 4$ GeV and $|y| < 1.5$, sizable Ξ_{bc} events about 1.7×10^7 and 3.5×10^9 per year can be produced for the center-of-mass energy $\sqrt{S} = 7$ TeV and $\sqrt{S} = 14$ TeV respectively. For experimental usage, the total and the interested differential cross-sections are estimated under some typical p_T - and y - cuts for the LHC detectors CMS, ATLAS and LHCb. Main uncertainties are discussed and a comparative study on the hadronic production of Ξ_{cc} , Ξ_{bc} and Ξ_{bb} at LHC are also presented.

PACS numbers: 12.38.Bx, 12.39.Jh, 13.60.Rj, 14.20.Lq, 14.20.Pt

Keywords: hadronic production, doubly heavy baryon, LHC

I. INTRODUCTION

The doubly heavy baryons, which represent a new type of objects in comparison with the ordinary baryons, were first predicted by Ref.[1]. These baryons shall offer a good platform for testing various theories and models, such as the quark model, the perturbative Quantum Chromodynamics (pQCD), the nonrelativistic QCD (NRQCD), the potential model and so on. Moreover, to know these baryons well can help us to understand the heavy-flavor physics, the weak interaction, the charge-parity violation, and etc.. A number of heavy baryons were discovered by several experiment collaborations, such as CLEO, Belle and BaBar, ARGUS, SELEX and CDF collaborations, a review on this point can be found in Refs.[2–4]. However, for the family of double-heavy baryons, only Ξ_{cc} has been observed and reported [5–8]. While due to their smaller production rate, few Ξ_{bc} and Ξ_{bb} have been observed. Even for Ξ_{cc} , its measured production rate and decay width are much larger than most of the theoretical predictions [9–18]. More data are needed to clarify the present situation.

The CERN Large Hadron Collider (LHC), which is designed to run with a high center-of-mass (C.M.) collision energy up to 14 TeV and a high luminosity up to $10^{-34} \text{cm}^{-2} \text{s}^{-1}$ [19], shall be of great help for the purpose. At the present, it is setting up for running with $\sqrt{S} = 7$ TeV and will result in an integrated luminosity of 10fb^{-1} after its first year of running. Taking into account the prospects of observation and measurement of doubly heavy baryons at LHC, it would be interesting to investigate the properties of these states. In the present paper, we shall first concentrate our attention on the hadronic production of Ξ_{bc} , and then make a comparative study with those of Ξ_{cc} and Ξ_{bb} .

The doubly heavy baryon can be regarded as a combination of the heavy diquark and a light quark [20]. The

dominant mechanism for the hadronic production of Ξ_{bc} baryon is the gluon-gluon fusion mechanism via the process $g + g \rightarrow \Xi_{bc} + \bar{b} + \bar{c}$. The gluon-gluon fusion mechanism includes 36 Feynman diagrams similar to the case of the Ξ_{cc} baryon production [9–15, 21, 22] and the B_c meson production [23–25], all of which can be schematically represented by Fig.(1), where k_1 and k_2 are two momenta for the initial gluons, q_{b2} and q_{c4} are momenta for the two outgoing \bar{b} and \bar{c} , P is the momentum of Ξ_{bc} . The intermediate (bc) -diquark pair can be in one of the four Fock states, i.e. $(bc)_{\bar{3}}[^3S_1]$, $(bc)_{\bar{6}}[^1S_0]$, $(bc)_{\bar{6}}[^3S_1]$ and $(bc)_{\bar{3}}[^1S_0]$ respectively. More definitely, according to Refs.[14, 21, 22], the hadronic production of Ξ_{bc} can be divided into three steps: the first step is the production of a $c\bar{c}$ -pair and a $b\bar{b}$ -pair that can be calculated by pQCD, since the intermediate gluon should be hard enough to form a heavy quark-antiquark pair. The second step is that the two heavy quarks fusion into a binding (bc) -diquark, and the third step is the fragmentation of such diquark into the desired baryon by grabbing a light quark and suitable number of gluons when needs. The second and the third steps are non-perturbative, which can be described by a universal matrix element within the NRQCD framework [26].

The paper is organized as follows. In Sec.II, we give the main idea in dealing with the Ξ_{bc} hadroproduction. Numerical results are presented in Sec.III. And in Sec.IV, we make a discussion on the main uncertainties for Ξ_{bc} hadroproduction and a comparison of the hadronic production of Ξ_{bc} , Ξ_{cc} and Ξ_{bb} . The final section is reserved for a summary.

II. CALCULATION TECHNOLOGY

Within the NRQCD framework, the total hadronic cross-section for the gluon-gluon fusion mechanism can be schematically written as the following factorization form

$$\sigma = F_{H_1}^g(x_1, \mu_F) F_{H_2}^g(x_2, \mu_F) \bigotimes \hat{\sigma}_{gg \rightarrow \Xi_{bc}}(x_1, x_2, \mu_F, \mu_R),$$

* wuxg@cqu.edu.cn

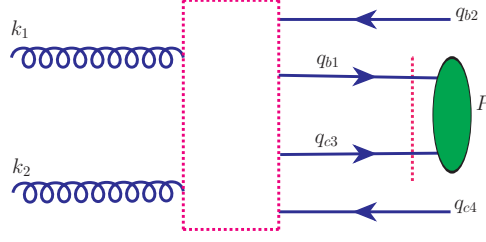


FIG. 1. Schematic diagram for the hadroproduction of Ξ_{bc} from the gluon-gluon fusion mechanism $g(k_1) + g(k_2) \rightarrow \Xi_{bc}(P) + \bar{b}(q_{b2}) + \bar{c}(q_{c2})$, where the dashed box stands for the hard interaction kernel.

where $F_H^i(x, \mu_F)$ (with $H = H_1$ or H_2 ; $x = x_1$ or x_2) is the distribution function of parton i in hadron H . μ_F is the factorization scale and μ_R is the renormalization scale, and for convenience, we take them to be the trans-

verse mass of Ξ_{bc} , i.e. $\mu_R = \mu_F = \sqrt{M_{\Xi_{bc}}^2 + p_T^2}$. $\hat{\sigma}_{gg \rightarrow \Xi_{bc}}$ stands for the cross-section for the gluon-gluon fusion subprocess, which can be expressed as [15, 18, 21],

$$\begin{aligned} \hat{\sigma}_{gg \rightarrow \Xi_{bc}} = & H(gg \rightarrow (bc)_{\bar{3}}[{}^3S_1]) \cdot h_3^{(bc)} + H(gg \rightarrow (bc)_{\mathbf{6}}[{}^1S_0]) \cdot h_1^{(bc)} + H(gg \rightarrow (bc)_{\bar{3}}[{}^1S_0]) \cdot h'_3{}^{(bc)} \\ & + H(gg \rightarrow (bc)_{\mathbf{6}}[{}^3S_1]) \cdot h'_1{}^{(bc)} + \dots, \end{aligned} \quad (1)$$

where the ellipsis stands for the terms in higher orders of v , v is the relative velocity between the constitute b and c quarks. $H(gg \rightarrow (bc)_{\bar{3},\mathbf{6}}[{}^3S_1])$ or $H(gg \rightarrow (bc)_{\bar{3},\mathbf{6}}[{}^1S_0])$ is the perturbative coefficient for producing (bc) -diquark in different spin and color configurations respectively. Four matrix elements: $h_1^{(bc)}$, $h_3^{(bc)}$, $h'_1{}^{(bc)}$ and $h'_3{}^{(bc)}$ characterize the transitions of the (bc) -diquark in $[{}^1S_0]_{\mathbf{6}}$, $[{}^3S_1]_{\bar{3}}$, $[{}^3S_1]_{\mathbf{6}}$, $[{}^1S_0]_{\bar{3}}$ spin and color configurations into Ξ_{bc} baryon respectively. $h_3^{(bc)}$ can be related to the wavefunction of the color anti-triplet diquark $(bc)_{\bar{3}}[{}^3S_1]$ as $h_3^{(bc)} = |\Psi_{bc}(0)|^2$. According to the discussions shown by Ref.[18], other matrix elements $h_1^{(bc)}$, $h'_1{}^{(bc)}$ and $h'_3{}^{(bc)}$ are of the same order in v as $h_3^{(bc)}$. Since all these matrix elements emerge as overall parameters, we can easily improve our numerical results when we know these matrix elements well. Naively, we take all of them to be $h_3^{(bc)}$ to do our estimation [18, 21, 22].

To derive analytical squared amplitude of the 36 Feynman diagrams for the hard subprocess is a tedious task, since it contains non-Abelian gluons and massive fermions. In Refs.[14, 24], the so-called improved helicity amplitude approach has been adopted to derive analytical expressions for the process at the amplitude level. And basing on the obtained sententious and analytical expressions, an effective generator GENXICC [21, 22] for simulating Ξ_{cc} , Ξ_{bc} and Ξ_{bb} events has been accomplished. Here we shall use GENXICC to make a detailed study on the hadronic production of Ξ_{bc} .

III. NUMERICAL RESULTS

To be consistent with the leading-order (LO) hard scattering amplitude, the LO parton distribution function (PDF) of CTEQ group, i.e. CTEQ6L [27], and the LO running α_s are adopted in doing the numerical calculation. And for other parameters we adopt the following values [10]:

$$\begin{aligned} m_c = 1.8 \text{ GeV}, \quad m_b = 5.1 \text{ GeV}, \\ M_{\Xi_{bc}} = 6.9 \text{ GeV}, \quad |\Psi_{bc}(0)|^2 = 0.065 \text{ GeV}^3. \end{aligned} \quad (2)$$

In TAB.I and TAB.II, we show the total cross sections for Ξ_{bc} with its (bc) -diquark in $(bc)_{\bar{3},\mathbf{6}}[{}^1S_0]$ and $(bc)_{\bar{3},\mathbf{6}}[{}^3S_1]$ states respectively. In these two tables, the results for the C.M. energies $\sqrt{S} = 7.0$ TeV and $\sqrt{S} = 14.0$ TeV are presented. Total cross sections with typical cuts for ATLAS, CMS and LHCb are adopted [28–30], e.g. the transverse momentum cut $p_{tcut} = 0, 2.5$ GeV and 4.0 GeV, and the rapidity cut $|y| < 1.5$ and $|y| < 2.5$ for ATLAS and CMS, and $1.9 < |\eta| < 4.9$ for LHCb are used for the estimation. For CMS, it usually adopts the pseudo-rapidity cut condition around $|\eta| < 2.5$, since the p_T - and y - differential distributions for the four diquark states $(bc)_n$ under the two cases of $|y| < 2.5$ and $|\eta| < 2.5$ are close in shape, and their corresponding total cross sections with pseudo-rapidity cut $|\eta| < 2.5$ are also close to those with rapidity cut $|y| < 2.5$, i.e. $\sigma_{|\eta| < 2.5}^n / \sigma_{|y| < 2.5}^n \sim 70\% - 85\%$, so to short the paper we take the same cut conditions for both ATLAS and CMS. Here the short notation $(bc)_n$ with (n=1,2,3,4) stands for $(bc)_{\bar{3}}[{}^1S_0]$, $(bc)_{\mathbf{6}}[{}^1S_0]$, $(bc)_{\bar{3}}[{}^3S_1]$ and $(bc)_{\mathbf{6}}[{}^3S_1]$ respectively.

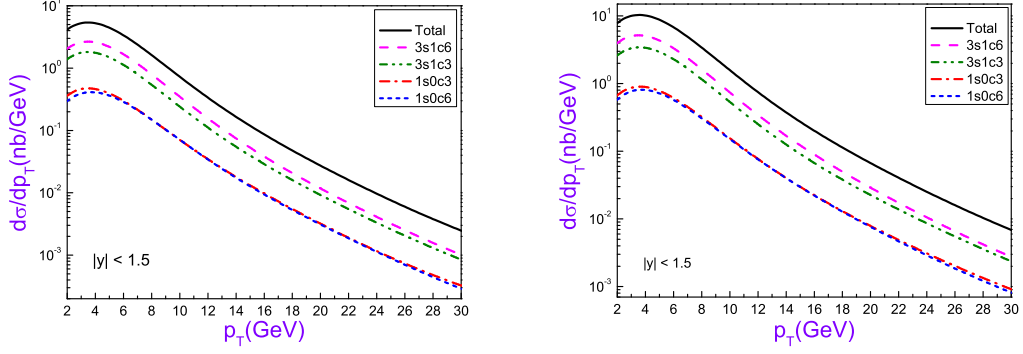


FIG. 2. p_T -distributions for Ξ_{bc} hadroproduction under ATLAS and CMS rapidity cut $|y| < 1.5$, where the left and the right diagrams are for $\sqrt{S} = 7$ TeV and $\sqrt{S} = 14$ TeV respectively. The solid, the dashed, the dash-dot-dot, the dash-dot and the short-dash lines stand for the total, that of $(bc)_6[{}^3S_1]$, $(bc)_3[{}^3S_1]$, $(bc)_3[{}^1S_0]$ and $(bc)_6[{}^1S_0]$ respectively.

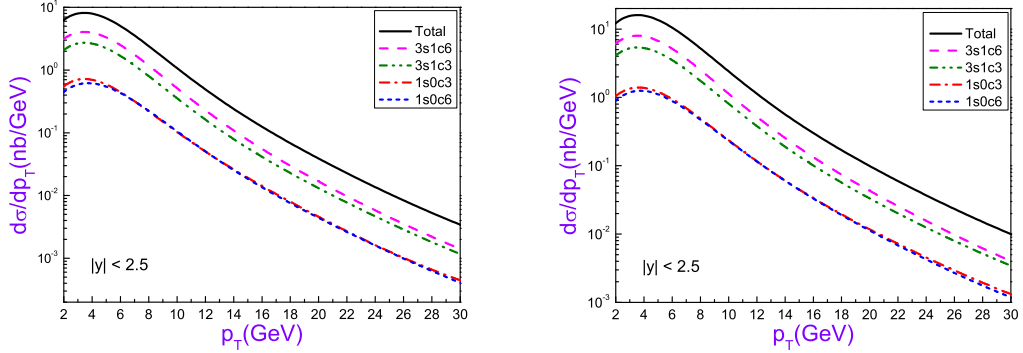


FIG. 3. p_T -distributions for Ξ_{bc} hadroproduction under ATLAS and CMS rapidity cut $|y| < 2.5$, where the left and the right diagrams are for $\sqrt{S} = 7$ TeV and $\sqrt{S} = 14$ TeV respectively. The solid, the dashed, the dash-dot-dot, the dash-dot and the short-dash lines stand for the total, that of $(bc)_6[{}^3S_1]$, $(bc)_3[{}^3S_1]$, $(bc)_3[{}^1S_0]$ and $(bc)_6[{}^1S_0]$ respectively.

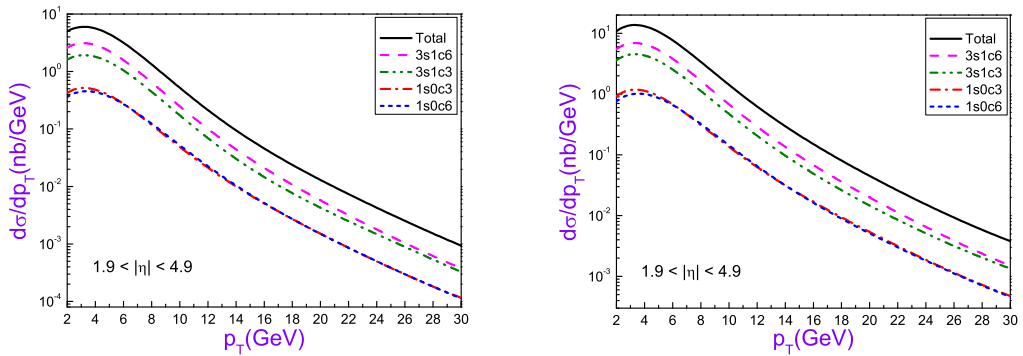


FIG. 4. p_T -distributions for Ξ_{bc} hadroproduction under LHCb pseudo-rapidity cut $1.9 < |\eta| < 4.9$, where the left and the right diagrams are for $\sqrt{S} = 7$ TeV and $\sqrt{S} = 14$ TeV respectively. The solid, the dashed, the dash-dot-dot, the dash-dot and the short-dash lines stand for the total, that of $(bc)_6[{}^3S_1]$, $(bc)_3[{}^3S_1]$, $(bc)_3[{}^1S_0]$ and $(bc)_6[{}^1S_0]$ respectively.

TABLE I. Hadronic cross section (in unit nb) for Ξ_{bc} at LHC with $\sqrt{S} = 7.0$ TeV. Three typical p_T cuts are adopted. As for the rapidity and pseudo-rapidity cut, we take $|y| < 1.5$ and $|y| < 2.5$ for CMS and ATLAS, and $1.9 < |\eta| < 4.9$ for LHCb.

-	-	-	LHC (CMS, ATLAS)		LHCb
-	y_{cut} or η_{cut}	NO cut	$ y < 1.5$	$ y < 2.5$	$1.9 \leq \eta \leq 4.9$
$(bc)_{\bar{3}}[{}^3S_1]$	0 GeV	20.90	10.82	16.21	11.12
-	2.5 GeV	16.01	8.363	12.49	7.941
-	4.0 GeV	10.72	5.674	8.446	4.886
$(bc)_6[{}^1S_0]$	0 GeV	5.120	2.618	3.938	2.689
-	2.5 GeV	4.062	2.094	3.142	2.006
-	4.0 GeV	2.853	1.489	2.227	1.307
$(bc)_6[{}^3S_1]$	0 GeV	31.70	16.03	24.20	17.09
-	2.5 GeV	24.09	12.30	18.52	12.17
-	4.0 GeV	15.97	8.276	12.42	7.441
$(bc)_{\bar{3}}[{}^1S_0]$	0 GeV	5.502	2.886	4.315	2.896
-	2.5 GeV	4.280	2.259	3.372	2.096
-	4.0 GeV	2.941	1.569	2.337	1.325

TABLE II. Hadronic cross section (in unit nb) for Ξ_{bc} at LHC with $\sqrt{S} = 14.0$ TeV. Three typical p_T cuts are adopted. As for the rapidity and pseudo-rapidity cut, we take $|y| < 1.5$ and $|y| < 2.5$ for CMS and ATLAS, and $1.9 < |\eta| < 4.9$ for LHCb.

-	-	-	LHC(CMS, ATLAS)		LHCb
-	y_{cut} or η_{cut}	NO cut	$ y < 1.5$	$ y < 2.5$	$1.9 < \eta < 4.9$
$(bc)_{\bar{3}}[{}^3S_1]$	0 GeV	47.24	21.70	33.43	25.85
-	2.5 GeV	36.55	16.92	26.04	19.17
-	4.0 GeV	24.92	11.70	17.95	12.34
$(bc)_6[{}^1S_0]$	0 GeV	11.55	5.259	8.112	6.250
-	2.5 GeV	9.255	4.243	6.537	4.822
-	4.0 GeV	6.607	3.067	4.713	3.269
$(bc)_6[{}^3S_1]$	0 GeV	70.67	31.80	49.19	38.89
-	2.5 GeV	54.29	24.65	38.07	28.74
-	4.0 GeV	36.59	16.85	25.97	18.36
$(bc)_{\bar{3}}[{}^1S_0]$	0 GeV	12.46	5.794	8.909	6.788
-	2.5 GeV	9.802	4.591	7.049	5.111
-	4.0 GeV	6.855	3.248	4.975	3.377

TABs.(I,II) show that all the four diquark states $(bc)_{\bar{3},6}[{}^1S_0]$ and $(bc)_{\bar{3},6}[{}^3S_1]$ can provide sizable contributions to Ξ_{bc} hadroproduction. Moreover, one may observe $\sigma_{(bc)_6[{}^3S_1]} > \sigma_{(bc)_{\bar{3}}[{}^3S_1]} > \sigma_{(bc)_{\bar{3}}[{}^1S_0]} \gtrsim \sigma_{(bc)_6[{}^1S_0]}$. And the total cross section for the scalar diquark states $(bc)_{\bar{3},6}[{}^1S_0]$ is about 20% of that of the vector diquark states $(bc)_{\bar{3},6}[{}^3S_1]$. Differential cross sections versus Ξ_{bc} - p_T are drawn in Figs.(2,3,4), where the results for the three typical rapidity or pseudo-rapidity cuts $|y| < 1.5$, $|y| < 2.5$ and $1.9 < |\eta| < 4.9$ are presented and these curves show the relative importance of the four diquark states clearly.

The LHC has been first running at $\sqrt{S} = 7.0$ TeV with luminosity $2.0 \times 10^{-32} cm^{-2} s^{-1}$ from 30th March 2010,

and its integrated luminosity is $10 fb^{-1}/yr$. Based on the total cross sections shown in TAB.I, one can estimate that about $1.7 \times 10^7 \Xi_{bc}$ events per year can be produced under the condition of $p_T > 4$ GeV and $|y| < 1.5$. When the C.M. energy and the luminosity are reached up to 14 TeV and $10^{-34} cm^{-2} s^{-1}$ as designed, then the integrated luminosity will be changed to $100 fb^{-1}/yr$, one can estimate that about $3.5 \times 10^9 \Xi_{bc}$ events per year can be produced under the condition of $p_T > 4$ GeV and $|y| < 1.5$.

Next, we draw the p_T - and y - distributions under some typical p_T - and y - cuts in Figs.(5,6), where each curve stands for the sum of all the four diquark states $(bc)_{\bar{3},6}[{}^1S_0]$ and $(bc)_{\bar{3},6}[{}^3S_1]$. The results for $\sqrt{S} = 7.0$

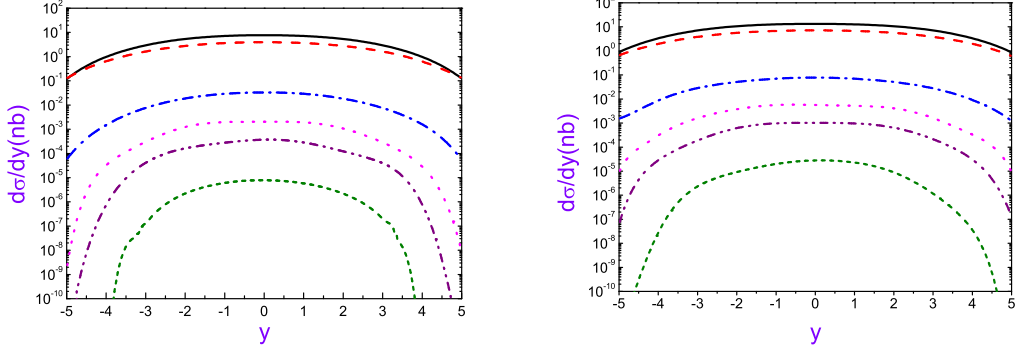


FIG. 5. The y -distributions for Ξ_{bc} production with various p_{Tcut} in LHC, where the left and the right diagrams are for $\sqrt{S} = 7.0$ TeV and $\sqrt{S} = 14.0$ TeV. The Solid line corresponds to the full production without p_{Tcut} , the dashed, the dash-dot, the dotted, the dash-dot-dot and the short dashed lines are for $p_{Tcut} = 4.0$ GeV, 20.0 GeV, 35.0 GeV, 50.0 GeV 100.0 GeV respectively. All the curves are the sum of all the four diquark states.

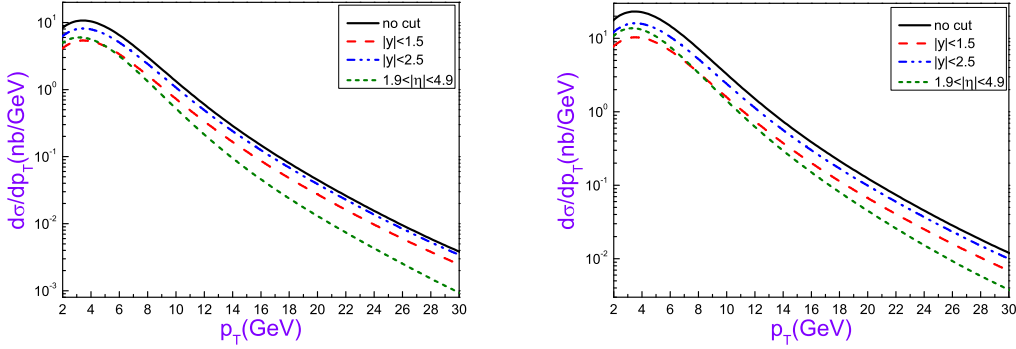


FIG. 6. The p_T -distributions for Ξ_{bc} production under various y - and η - cut, where the left and the right diagrams are for $\sqrt{S} = 7$ TeV and $\sqrt{S} = 14$ TeV respectively. The solid, the dashed, the dash-dot-dot and the short dash lines stand for no-cut, $|y| < 1.5$, $|y| < 2.5$ and $1.9 < |\eta| < 4.9$ respectively. All the curves are the sum of all the four diquark states.

TeV and $\sqrt{S} = 14.0$ TeV are presented accordingly. Firstly, as shown by Fig.(5), there is an obvious platform within the region of $|y| \lesssim 3.0$, where dominant contributions to the cross section are there. To show this point clearly, we define a ratio $R_c^{p_{Tcut}} = [\sigma_{|y|<c}/\sigma_{tot}]_{p_{Tcut}}$, where σ_{tot} stands for the total cross section without y -cut and c stands for some particular value. Then we obtain $R_{1.5}^{4GeV} = 52\%$ and $R_{2.5}^{4GeV} = 78\%$ for $\sqrt{S} = 7.0$ TeV, and $R_{1.5}^{4GeV} = 47\%$ and $R_{2.5}^{4GeV} = 72\%$ for $\sqrt{S} = 14.0$ TeV. Secondly, as shown by Fig.(6), the p_T -distribution under the case of $1.9 < |\eta| < 4.9$ drops faster than the cases with other y -cuts, especially in the large p_T regions. This implies that if the same larger p_T cut (e.g. $p_t > 10$ GeV) is imposed at the colliders ¹, ATLAS and CMS are better than LHCb for studying Ξ_{bc} properties, since

more events can be produced and measured at ATLAS and CMS.

IV. DISCUSSIONS

A. Main uncertainties for Ξ_{bc} hadroproduction

To be more useful experimentally, we make a simple discussion on the uncertainties for Ξ_{bc} hadroproduction. For the present LO estimation, the uncertainty sources include the non-perturbative matrix elements, the factorization scale μ_F , the constitute quark masses m_b and m_c , PDF and etc..

¹ Since the events move very close to the beam direction cannot be

detected by the detectors directly, so such kind of events cannot be utilized for experimental studies in common cases.

Numerically, it is found that similar to the hadronic production of B_c , B_s and Ξ_{cc} that have been done in the literature, the LO PDFs like MRST2001L [31] and CETQ6L [27] only lead to small difference to the total cross section that is less than 15%. So we shall fix the PDF to be CTEQ6L to do our discussion. Moreover, all the non-perturbative matrix elements emerge as overall parameters, then we can easily improve our numerical results when we know these matrix elements well. In the following, we shall concentrate our attention on the uncertainties caused by the factorization scale μ_F , and the constituent quark masses m_b and m_c .

In TAB.III, we present the total cross sections for two typical factorization scales, i.e. type A: $\mu_F = \sqrt{\hat{s}}/4$ with $\hat{s} = x_1 x_2 S$, and type B: $\mu_F = \sqrt{M_{\Xi_{bc}}^2 + p_T^2}$. Other parameters are fixed to be their center values. Here, $p_{Tcut} = 4.0$ GeV, and the rapidity cut $|y| < 1.5$ and $|y| < 2.5$ for ATLAS and CMS, and $1.9 < |\eta| < 4.9$ for LHCb are adopted for the estimation. It is found that the cross section differences caused by these two factorization scales is about 25% – 30% for the four diquark states $(bc)\bar{3}_6[{}^1S_0]$ and $(bc)\bar{3}_6[{}^3S_1]$ respectively, which is a comparatively large effect.

Next, we investigate the uncertainties of m_b and m_c in ‘a factorization way’. More explicitly, when focusing on the uncertainty from m_b , we let it be a basic input varying in a possible range $m_b = 5.1 \pm 0.20$ GeV with all the other parameters being fixed to their center values, e.g. $m_c = 1.80$ GeV, $M_{\Xi_{bc}} = m_b + m_c$ and $\mu_F = \sqrt{M_{\Xi_{bc}}^2 + p_T^2}$. Similarly, when discussing the uncertainty caused by m_c , we vary m_c within the region of $m_c = 1.8 \pm 0.10$ GeV with all the other parameters being fixed to be their center values.

We present the total cross sections for Ξ_{bc} with varying m_b or m_c for C.M. energies $\sqrt{S} = 7.0$ TeV and $\sqrt{S} = 14.0$ TeV in TAB.IV and TAB.V. Here, $p_{Tcut} = 4.0$ GeV, the rapidity cut $|y| < 1.5$ and $|y| < 2.5$ for ATLAS and CMS, and $1.9 < |\eta| < 4.9$ for LHCb are adopted for the estimation. Quantitatively, it can be found that the total cross sections decreases with the increment of m_b or m_c , which can be roughly explained by the smaller production phase space for larger quark masses. And from TAB.IV and TAB.V, one may observe that the cross sections are more sensitive to the value of m_c than m_b . When m_b increases or decreases by the step of 0.2 GeV, the cross section of Ξ_{bc} changes around 8% – 10% for the four diquark states $(bc)\bar{3}_6[{}^1S_0]$ and $(bc)\bar{3}_6[{}^3S_1]$. While for the case of m_c , when m_c increases or decreases by step of 0.1 GeV, the cross section of Ξ_{bc} decreases or increases by 15% – 20% for the four diquark states $(bc)\bar{3}_6[{}^1S_0]$ and $(bc)\bar{3}_6[{}^3S_1]$.

B. A comparison of the hadronic production of Ξ_{cc} , Ξ_{bc} and Ξ_{bb}

To be useful reference, we make a comparison of the hadronic production of Ξ_{cc} , Ξ_{bc} and Ξ_{bb} at LHC. The total cross sections are presented in TAB.VI, where $[{}^3S_1]$ and $[{}^1S_0]$ stand for the results for the diquark in spin-triplet and spin-singlet states respectively. More explicitly, for hadronic production of Ξ_{cc} , one needs to consider the contributions from the two diquark states $(cc)\bar{6}[{}^1S_0]$ and $(cc)\bar{3}[{}^3S_1]$. As for hadronic production of Ξ_{bb} , one needs to consider the contributions from the two diquark states $(bb)\bar{6}[{}^1S_0]$ and $(bb)\bar{3}[{}^3S_1]$. While for the case of Ξ_{bc} , one needs to consider the contributions from the four diquark states $(bc)\bar{3}_6[{}^1S_0]$ and $(bc)\bar{3}_6[{}^3S_1]$.

From TAB.VI, one can see that the total cross section of Ξ_{bc} is at the same order of that of Ξ_{cc} , i.e. it is about 40% and 44% of that of Ξ_{cc} for $\sqrt{S} = 7$ TeV and $\sqrt{S} = 14$ TeV respectively. While, the total cross section of Ξ_{bb} is only 1.5% and 2% of that of Ξ_{cc} for $\sqrt{S} = 7$ TeV and $\sqrt{S} = 14$ TeV respectively. Then, similar to the case of Ξ_{cc} that has been measured by the SELEX experiment at TEVATRON [5, 6], it would be possible for Ξ_{bc} be fully studied at LHC.

We draw the y - and p_T - distributions for Ξ_{cc} , Ξ_{bc} and Ξ_{bb} production under the case of $p_T > 4$ GeV and $|y| < 1.5$ in Figs.(7,8), where each curve includes the sum of all the mentioned S-wave diquark states. Fig.(8) shows that production cross section of Ξ_{bc} is smaller than that of Ξ_{cc} in the lower p_T region, however it will dominant over that of Ξ_{cc} when $p_T \gtrsim 9$ GeV.

V. SUMMARY

We have analyzed the hadronic production of Ξ_{bc} via the dominant gluon-gluon fusion mechanism at LHC with the center-of-mass energy $\sqrt{S} = 7$ TeV and $\sqrt{S} = 14$ TeV respectively. For experimental usage, the total and the interested differential cross-sections have been estimated under typical cut conditions for the LHC detectors CMS, ATLAS and LHCb.

Numerical results show that about 1.7×10^7 and 3.5×10^9 Ξ_{bc} events per year can be produced for $\sqrt{S} = 7$ TeV and $\sqrt{S} = 14$ TeV under the condition of $p_T > 4$ GeV and $|y| < 1.5$. This indicates that Ξ_{bc} can be observed and studied at LHC. Main uncertainties for the estimation have been discussed and a comparative study on the hadronic production of Ξ_{cc} , Ξ_{bc} and Ξ_{bb} at LHC with $\sqrt{S} = 7$ TeV and $\sqrt{S} = 14$ TeV have also been presented. As for the total production cross section under the case of $p_T < 4$ GeV, we have $\sigma_{\Xi_{bc}} < \sigma_{\Xi_{cc}}$, however the differential cross-section of Ξ_{bc} will dominant over that of Ξ_{cc} when $p_T \gtrsim 9$ GeV.

In the above, we have not distinguished the light components in the baryon. More subtly, as for the production of Ξ_{bc} , after the formation of the heavy (bc) -diquark, it will grab a light anti-quark (with gluons when necessary)

TABLE III. Hadronic cross section (in unit nb) of Ξ_{bc} at LHC for two typical energy scales A and B. $p_{Tcut} = 4.0$ GeV, $|y| < 1.5$ and $|y| < 2.5$ for CMS and ATLAS, and $1.9 < |\eta| < 4.9$ for LHCb are adopted for the estimation.

-	μ_F	A	B	A	B	A	B
-	y_{cut} or η_{cut}	$ y < 1.5$		$ y < 2.5$		$1.9 < \eta < 4.9$	
-	C.M. Energy						
$(bc)_{\bar{3}}[{}^3S_1]$	$\sqrt{S} = 7.0$ TeV	3.957	5.674	5.889	8.446	3.403	4.886
-	$\sqrt{S} = 14.0$ TeV	8.477	11.70	12.99	17.95	8.893	12.34
$(bc)_6[{}^1S_0]$	$\sqrt{S} = 7.0$ TeV	1.078	1.489	1.612	2.227	0.939	1.307
-	$\sqrt{S} = 14.0$ TeV	2.298	3.067	3.529	4.713	2.432	3.269
$(bc)_6[{}^3S_1]$	$\sqrt{S} = 7.0$ TeV	6.135	8.276	9.200	12.42	5.471	7.441
-	$\sqrt{S} = 14.0$ TeV	12.90	16.85	19.85	25.97	13.94	18.36
$(bc)_{\bar{3}}[{}^1S_0]$	$\sqrt{S} = 7.0$ TeV	1.104	1.569	1.646	2.337	0.941	1.325
-	$\sqrt{S} = 14.0$ TeV	2.360	3.248	3.617	4.975	2.455	3.377

TABLE IV. Hadronic cross section (in unit nb) of Ξ_{bc} at LHC with varying $m_b \in [4.9, 5.3]$ GeV. Other parameters are fixed to be their center values. $p_{Tcut} = 4.0$ GeV, $|y| < 1.5$ and $|y| < 2.5$ for CMS and ATLAS, and $1.9 < |\eta| < 4.9$ for LHCb are adopted for the estimation.

-	y_{cut} or η_{cut}	$ y < 1.5$	$ y < 2.5$	$1.9 < \eta < 4.9$
-	C.M. Energy			
$(bc)_{\bar{3}}[{}^3S_1]$	$\sqrt{S} = 7.0$ TeV	$5.674^{+0.593}_{-0.519}$	$8.446^{+0.905}_{-0.769}$	$4.886^{+0.526}_{-0.443}$
-	$\sqrt{S} = 14.0$ TeV	$11.70^{+1.15}_{-1.02}$	$17.95^{+1.76}_{-1.58}$	$12.34^{+1.24}_{-1.10}$
$(bc)_6[{}^1S_0]$	$\sqrt{S} = 7.0$ TeV	$1.489^{+0.137}_{-0.122}$	$2.227^{+0.207}_{-0.185}$	$1.307^{+0.123}_{-0.109}$
-	$\sqrt{S} = 14.0$ TeV	$3.067^{+0.265}_{-0.237}$	$4.713^{+0.416}_{-0.368}$	$3.269^{+0.292}_{-0.260}$
$(bc)_6[{}^3S_1]$	$\sqrt{S} = 7.0$ TeV	$8.276^{+0.868}_{-0.761}$	$12.42^{+1.31}_{-1.16}$	$7.441^{+0.797}_{-0.701}$
-	$\sqrt{S} = 14.0$ TeV	$16.85^{+1.67}_{-1.49}$	$25.97^{+2.58}_{-2.35}$	$18.36^{+1.83}_{-1.67}$
$(bc)_{\bar{3}}[{}^1S_0]$	$\sqrt{S} = 7.0$ TeV	$1.569^{+0.167}_{-0.148}$	$2.337^{+0.250}_{-0.225}$	$1.325^{+0.144}_{-0.128}$
-	$\sqrt{S} = 14.0$ TeV	$3.248^{+0.319}_{-0.300}$	$4.975^{+0.494}_{-0.449}$	$3.377^{+0.334}_{-0.309}$

from the hadron collision environment to form a colorless double heavy baryon with the relative possibility for the light quark as $u : d : s \simeq 1 : 1 : 0.3$ [32], i.e. to form the baryons Ξ_{bc}^+ , Ξ_{bc}^0 or Ω_{bc}^0 . More precisely, when the diquark (bc) is produced, it will fragment into Ξ_{bc}^+ with 43% probability, Ξ_{bc}^0 with 43% probability and Ω_{bc}^+ with 14% probability accordingly. If enough Ξ_{bc} events can be accumulated at LHC, then one may have chances to study the $\Xi_{bc}^{+,0}$ or Ω_{bc}^0 separately from their decay products.

Acknowledgments: This work was supported in part by the Fundamental Research Funds for the Central Universities under Grant No.CDJXS11102209, by Natural Science Foundation of China under Grant No.10805082 and No.11075225 and by Natural Science Foundation Project of CQ CSTC under Grant No.2008BB0298.

TABLE V. Hadronic Cross section (in unit nb) of Ξ_{bc} at LHC with varying $m_c \in [1.7, 1.9]$ GeV. Other parameters are fixed to be their center values. $p_{Tcut} = 4.0$ GeV, $|y| < 1.5$ and $|y| < 2.5$ for CMS and ATLAS, and $1.9 < |\eta| < 4.9$ for LHCb are adopted for the estimation.

-	y_{cut} or η_{cut}	$ y < 1.5$	$ y < 2.5$	$1.9 < \eta < 4.9$
	C.M. Energy			
$(bc)_{\bar{3}}[{}^3S_1]$	$\sqrt{S} = 7.0$ TeV	$5.674^{+1.138}_{-0.893}$	$8.446^{+1.704}_{-1.330}$	$4.886^{+1.001}_{-0.128}$
	$\sqrt{S} = 14.0$ TeV	$11.70^{+2.31}_{-1.80}$	$17.95^{+3.54}_{-2.79}$	$12.34^{+2.45}_{-1.96}$
$(bc)_6[{}^1S_0]$	$\sqrt{S} = 7.0$ TeV	$1.489^{+0.336}_{-0.260}$	$2.227^{+0.506}_{-0.389}$	$1.307^{+0.302}_{-0.231}$
	$\sqrt{S} = 14.0$ TeV	$3.067^{+0.683}_{-0.525}$	$4.713^{+1.049}_{-0.807}$	$3.269^{+0.733}_{-0.570}$
$(bc)_6[{}^3S_1]$	$\sqrt{S} = 7.0$ TeV	$8.276^{+1.611}_{-1.282}$	$12.42^{+2.41}_{-1.93}$	$7.441^{+1.468}_{-1.163}$
	$\sqrt{S} = 14.0$ TeV	$16.85^{+3.20}_{-2.56}$	$25.97^{+4.95}_{-3.98}$	$18.36^{+3.53}_{-2.85}$
$(bc)_{\bar{3}}[{}^1S_0]$	$\sqrt{S} = 7.0$ TeV	$1.569^{+0.307}_{-0.247}$	$2.337^{+0.458}_{-0.369}$	$1.325^{+0.278}_{-0.212}$
	$\sqrt{S} = 14.0$ TeV	$3.248^{+0.627}_{-0.506}$	$4.975^{+0.967}_{-0.777}$	$3.377^{+0.658}_{-0.541}$

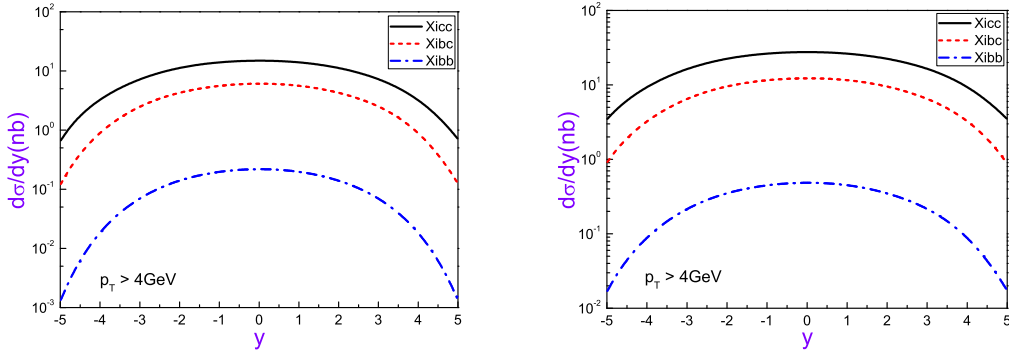


FIG. 7. The y -distributions for Ξ_{cc} , Ξ_{bc} and Ξ_{bb} production with $p_T > 4$ GeV in LHC, where the left and the right diagrams are for $\sqrt{S} = 7.0$ TeV and $\sqrt{S} = 14.0$ TeV. The Solid, the short dash and the dash-dot lines are for Ξ_{cc} , Ξ_{bc} and Ξ_{bb} respectively. All the curves are the sum of all the s-wave diquark states.

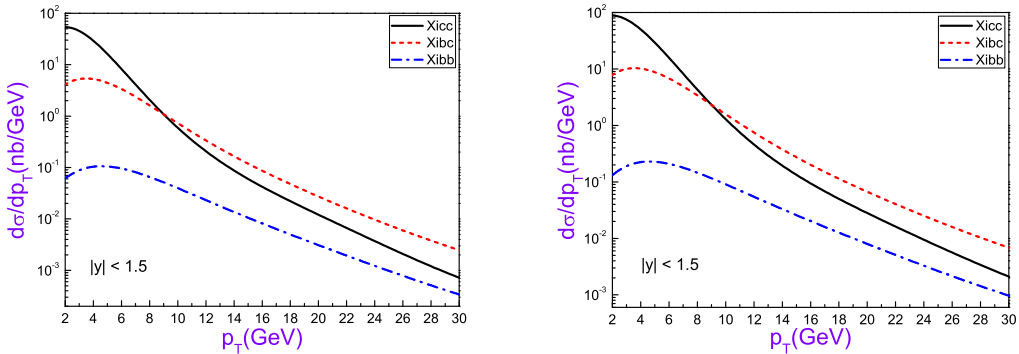


FIG. 8. The p_T -distributions for Ξ_{cc} , Ξ_{bc} and Ξ_{bb} production with rapidity cut condition $|y| < 1.5$ in LHC, where the left and the right diagrams are for $\sqrt{S} = 7.0$ TeV and $\sqrt{S} = 14.0$ TeV. The Solid, the short dash and the dash-dot lines are for Ξ_{cc} , Ξ_{bc} and Ξ_{bb} respectively. All the curves are the sum of all the s-wave diquark states.

TABLE VI. Comparison of the total cross section (in unit nb) for the hadronic production of Ξ_{cc} , Ξ_{bc} and Ξ_{bb} at $\sqrt{S} = 7.0$ TeV and $\sqrt{S} = 14.0$ TeV, where $[^3S_1]$ and $[^1S_0]$ stand for the combined results for the diquark in spin-triplet and spin-singlet states respectively. In the calculations, we adopt $p_T > 4$ GeV and $|y| < 1.5$.

-	Ξ_{cc}		Ξ_{bc}		Ξ_{bb}	
-	$\sqrt{S} = 7.0\text{TeV}$	$\sqrt{S} = 14.0\text{TeV}$	$\sqrt{S} = 7.0\text{TeV}$	$\sqrt{S} = 14.0\text{TeV}$	$\sqrt{S} = 7.0\text{TeV}$	$\sqrt{S} = 14.0\text{TeV}$
$[^3S_1]$	38.11	69.40	16.7	28.55	0.503	1.137
$[^1S_0]$	9.362	17.05	3.72	6.315	0.100	0.226
Total	47.47	86.45	20.42	34.87	0.603	1.363

-
- [1] S. Fleck, B. Silvestre-Brac and J.M. Richard, Phys.Rev. D**38**, 1519(1988).
 - [2] E. Klempt, J.M. Richard, Rev.Mod.Phys.**82**, 1095 (2010).
 - [3] N. Brambilla *et al.*, Quarkonium Working Group, Published as CERN Yellow Report, CERN-2005-005, arXiv: 0412158[hep-ph].
 - [4] N. Brambilla, *et al.*, Quarkonium Working Group, arXiv:1010.5827.
 - [5] M. Mattson *et al.*, SELEX Collaboration, Phys. Rev. Lett. **89**, 112001(2002).
 - [6] A. Ocherashvili *et al.*, SELEX Collaboration, Phys.Lett. B**628**, 18(2005).
 - [7] R. Chistov *et al.*, Belle Collaboration, Phys. Rev. Lett.**97**, 162001 (2006).
 - [8] B. Aubert *et al.*, BABAR Collaboration, Phys. Rev. D**74**, 011103 (2006).
 - [9] M. Moinester, Z.Phys. A**355**, 349(1996).
 - [10] S.P. Baranov, Phys.Rev. D**54**, 3228(1996).
 - [11] A.V. Berezhnoy, V.V. Kiselev and A.K. Likhoded, Phys.At.Nucl.**59**, 870(1996); Sov.J.Nucl.Phys. **59**, 909(1996).
 - [12] A.V. Berezhnoy, V.V. Kiselev, A.K. Likhoded and A.I. Onishchenko, Phys.Rev. D**57**, 4385(1998).
 - [13] V.V. Kiselev and A.K. Likhoded, Phys. Usp. **45**, 455 (2002).
 - [14] Chao-Hsi Chang, Cong-Feng Qiao, Jian-Xiong Wang and Xing-Gang Wu, Phys.Rev. D**73**, 094022(2006).
 - [15] Chao-Hsi Chang, Jian-Ping Ma, Cong-Feng Qiao, Xing-Gang Wu, J.Phys. G**34**, 845(2007).
 - [16] A.F. Falk, M. Luke, M.J. Savage and M.B. Wise, Phys.Rev. D **49**, 555(1994).
 - [17] M.A. Doncheski, J. Steegborn, and M.L. Stong, Phys. Rev. D**53**, 1247 (1996).
 - [18] J.P. Ma and Z.G. Si, Phys. Lett. B**568**, 135(2003).
 - [19] L. Evans and P. Bryant, JINST **3**, S08001 (2008).
 - [20] M. Ida and R. Kobayashi, Prog.Theor.Phys. **36**, 846(1966); D.B. Lichtenberg and L.J. Tassie, Phys.Rev. **155**, 1601(1967).
 - [21] Chao-Hsi Chang, Jian-Xiong Wang and Xing-Gang Wu, Comput.Phys.Commun.**177**, 467(2007).
 - [22] Chao-Hsi Chang, Jian-Xiong Wang and Xing-Gang Wu, Comput.Phys.Commun.**181**, 1144(2010).
 - [23] Chao-Hsi Chang and Yu-Qi Chen, Phys.Rev. D**48**, 4086(1993); Chao-Hsi Chang, Yu-Qi Chen, Guo-Ping Han and Hong-Tan Jiang, Phys.Lett. B**364**, 78(1995); Chao-Hsi Chang, Xing-Gang Wu, Eur.Phys.J. C**38**, 267(2004).
 - [24] Chao-Hsi Chang, Chafik Driouich, Paula Eerola and Xing-Gang Wu, Comput.Phys. Commun. **159**, 192 (2004); Chao-Hsi Chang, Jian-Xiong Wang and Xing-Gang Wu, Comput.Phys. Commun. **174**, 241 (2006); Chao-Hsi Chang, Jian-Xiong Wang and Xing-Gang Wu, Comput.Phys. Commun. **175**, 624 (2006).
 - [25] A.V. Berezhnoy, V.V. Kiselev and A.K. Likhoded, Z.Phys. A**356**, 79(1996); A.V. Berezhnoy, A.K. Likhoded and M.V. Shevlyagin, Phys.At. Nucl. **58**, 1732(1995).
 - [26] G.T. Bodwin, E. Braaten and G.P. Lepage, Phys. Rev. D **51**, 1125 (1995); Erratum Phys. Rev. D **55**, 5853 (1997).
 - [27] H. L. Lai *et al.*, J. High Energy Phys.**0207**, 012(2002).
 - [28] ATLAS Collaboration, CERN-LHCC-99-014; CERN-LHCC-99-015.
 - [29] R. Adolphy, *et al.*, CMS Collaboration, JINST **3**, S08004(2008).
 - [30] A.A. Alves, *et al.*, LHCb Collaboration, JINST **3**, S08005(2008).
 - [31] A.D. Martin, R.G. Robert, W.J. Stirling and R.S. Thorne, Eur.Phys.J. C**23**, 73(2002).
 - [32] T. Sjostrand, S. Mrenna and P. Skands, JHEP **0605**, 026(2006).